the Fourier transform of the EO-signal is shown in Fig. 3. To correct the frequency response for the effect of finite duration of the optical sampling and excitation pulse, the Fourier transforms of their measured autocorrelation traces are used. A further effect on the system response results from the finite transit time of the sampling pulse in the electro-optically active InP substrate. Its response characteristic is calculated by accounting for the spatial distribution of the electric field of the CPW line, assuming quasi-TEM behaviour of the propagating signal. The resulting frequency response of the EO-sampling system as well as the corrected response of the detector are shown in Fig. 3. A 3dB bandwidth of 70GHz results from the corrected response characteristic. The comparison of the corrected response with the RC-limited response (also shown in Fig. 3), which is obtained from the capacitance (29fF) and series resistance (5Ω) of the detector when connected to a 50Ω transmission line, shows that, in the frequency range 120 and 170GHz, the response is dominated by the RC-effect. Moreover, the comparison indicates that the transit-time limited bandwidth of the devices exceeds 150GHz. The corrected response slightly exceeds the RC-limit at very high frequencies in Fig. 3. This may be attributed to the uncertainty of the correction procedure, which is estimated to be ±0.5dB.

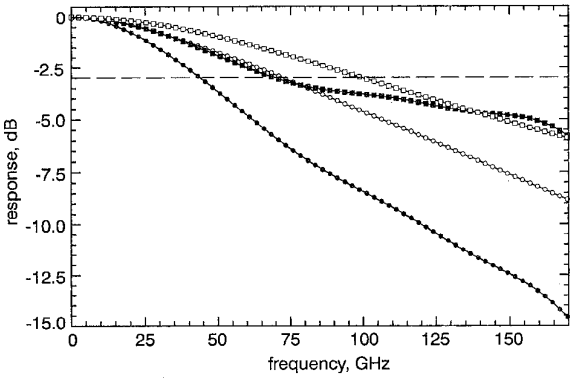

Fig. 3 *Frequency response characteristics*

■ corrected response
● uncorrected response
○ response of measuring system
□ RC limited response

Typically, the dark currents of the devices range between 1 and 2nA at 2V bias. The CW quantum efficiency of uncoated devices at 1.55 and 1.3μm is found to be 3.5 and 10%, respectively. The application of a silicon nitride AR coating leads to an enhanced efficiency of 6.7 and 17%, respectively. Note that the behaviour of the efficiency does not obey the geometric-optics approximation. Rather, its treatment requires the application of exact diffraction theory [4]. The polarisation dependence of the quantum efficiency is found to be < 0.2dB. Moreover, the AR coating gives rise to a larger capacitance of 40fF due to the increase in the effective dielectric constant. Thus, preserving the bandwidth of 70GHz with AR coated devices will require a reduction of the active area by ~30%. As recently demonstrated in conjunction with InGaAs MSM detectors [6], a drastic improvement of the quantum efficiency without a significant loss to bandwidth performance can be achieved by rear illumination in combination with resonant cavity enhanced (RCE) absorption. Such an RCE configuration is expected to result in a quantum efficiency of ~40% at 1.55μm.

Conclusion: Front-side illuminated 14μm active area diameter InGaAs photodetectors for high-speed and polarisation-insensitive operation have been fabricated. The devices possess 0.2μm feature size finger electrodes with a semicircular shape. A pulse response time of 3.8ps at 2V bias has been measured by EO-sampling at 1.55μm wavelength. The corrected frequency response exhibits a 3dB bandwidth of 70GHz.

Acknowledgments: The authors thank A. Strittmatter and K. Schatke for epitaxial growth, Th. Engel for his assistance in device fabrication, and D. Huhse for providing the 1.55μm optical pulse source. This work was supported in part by the German Research Foundation (DFG).

20 May 1998
Electronics Letters Online no: 19980992

E. Dröge, E.H. Böttcher and D. Bimberg (*Institut für Festkörperphysik I, Technische Universität Berlin, Hardenbergstraße 36, D-10623 Berlin, Germany*)

O. Reimann (*Department of Electromagnetic Theory, Technical University of Brandenburg, Karl-Marx-Straße 17, D-03044 Cottbus, Germany*)

R. Steingrüber (*Heinrich-Hertz-Institut für Nachrichtentechnik Berlin GmbH, Einsteinufer 37, D-10587 Berlin, Germany*)

References

1 BÖTTCHER, E.H., DRÖGE, E., BIMBERG, D., UMBACH, A., and ENGAL, H.: 'Ultra-wide-band (> 40GHz) submicron InGaAs metal-semiconductor-metal photodetectors', *IEEE Photonics Technol. Lett.*, 1996, **8**, pp. 1226–1228

2 SOOLE, J.B.D., and SCHUMACHER, H.: 'InGaAs metal-semiconductor-metal photodetectors for long wavelength optical communications', *IEEE J. Quantum Electron.*, 1991, **27**, pp. 737–752

3 HIERONYMI, F., BÖTTCHER, E.H., DRÖGE, E., KUHL, D., KOLLAKOWSKI, S., and BIMBERG, D.: 'Large-area low-capacitance InP/InGaAs MSM photodetectors for high-speed operation under front and rear illumination', *Electron. Lett.*, 1994, **30**, pp. 1247–1248

4 BÖTTCHER, E.H., DRÖGE, E., STRITTMATTER, A., and BIMBERG, D.: 'Polarisation-insensitive high-speed InGaAs metal-semiconductor-metal photodetectors', *Electron. Lett.*, 1997, **33**, pp. 912–914

5 REIMANN, O., HUHSE, D., DRÖGE, E., BÖTTCHER, E.H., and BIMBERG, D.: 'Semiconductor laser based electro-optical sampling system for direct probing at 1.55μm wavelength', to be published in *IEEE Photonics Technol. Lett.*

6 STRITTMATTER, A., KOLLAKOWSKI, S., DRÖGE, E., BÖTTCHER, E.H., and BIMBERG, D.: 'High-speed, high efficiency resonant-cavity-enhanced InGaAs MSM photodetectors', *Electron. Lett.*, 1996, **32**, pp. 1231–1232

Long wavelength velocity-matched distributed photodetectors for RF fibre optic links

T. Chau, L. Fan, D.T.K. Tong, S. Mathai, M.C. Wu, D.L. Sivco and A.Y. Cho

An InP-based long wavelength velocity-matched distributed photodetector with metal-semiconductor-metal photodiodes is experimentally demonstrated. A 3dB bandwidth of 18GHz and an external quantum efficiency of 0.42A/W have been achieved.

Introduction: High power, high frequency photodetectors are a key component for high performance microwave fibre optic links [1 – 3]. High optical power in externally modulated links can greatly enhance the link gain, signal-to-noise ratio, and the spurious-free dynamic range [4]. It is also very useful for millimeter-wave generation by photomixing. Previously, we have reported a GaAs/AlGaAs velocity-matched distributed photodetector (VMDP) operating at 860nm wavelength, and demonstrated its potential for high saturation photocurrent [1]. For applications in RF photonic systems, however, InP-based long-wavelength photodetectors operating at 1.3 or 1.55μm are required. The successful fabrication of a long-wavelength VMDP is first reported in [5]. In this Letter, we report on the experimental results and RF performance of the InGaAs/InAlGaAs/InP VMDP.

Device structure and fabrication: The schematic structure of the VMDP is illustrated in Fig. 1*a*. Active metal-semiconductor-metal (MSM) photodiodes are periodically distributed on top of a passive optical waveguide. The optical signal is evanescently coupled from the passive waveguide to the active MSM photodiodes. Photocurrents generated from the MSM photodiodes are added in phase through a 50Ω coplanar strip (CPS) microwave transmission line that is velocity-matched to the optical waveguide. The MSM photodiodes serve two functions: generating photocurrents and providing the periodic capacitance loading needed for velocity matching. The VMDP design allows the passive waveguide, the

active photodiodes, and the microwave coplanar strips to be independently optimised. The active MSM photodiodes consist of an InGaAs absorption layer, InGaAs/InAlAs graded superlattice layers, an InAlAs Schottky-barrier enhancement layer, and a Ti/Au contact with 200Å/2000Å thickness. The fabrication process is as follows: first, Ti/Au interdigitated fingers with 1.5μm width and 0.5μm spacing are patterned using standard photolithography and liftoff techniques, then active mesas for individual photodiodes are defined by wet etching down to the InAlAs upper cladding II. Fig. 1*b* shows the cross-section of the VMDP after mesa etching. A passive ridge waveguide with a ridge height of 0.1μm is employed to connect the photodiodes. After mesa and waveguide etching, the CPS microwave transmission line is patterned using a standard liftoff technique.

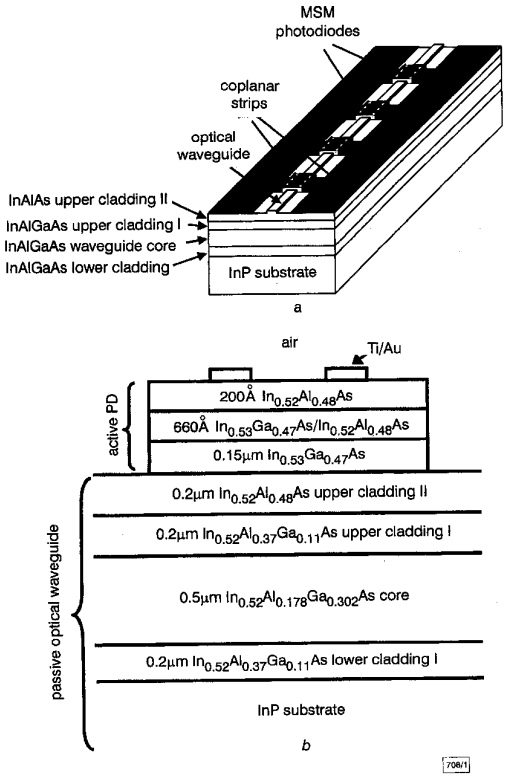

Fig. 1 *Schematic structure of long-wavelength VMDP and cross-section after mesa etching*

a Schematic structure of VMDP
b Schematic cross-section of VMDP after mesa etching

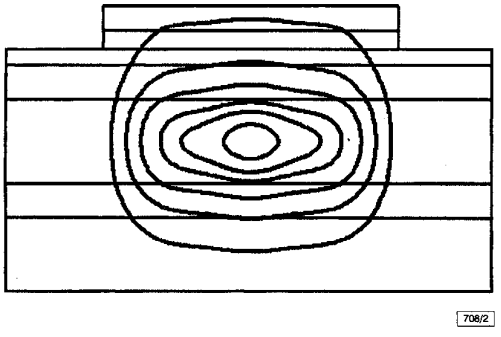

Fig. 2 *Contour plot of fundamental mode field amplitude in photodiode region using BPM simulation*

See Fig. 1 for detailed layer structure

The beam propagation method (BPM) is used to design and simulate the optical performance of the VMDP. A large-core optical waveguide is employed to reduce the coupling loss between the passive waveguide and the photodiode region as well as to reduce the optical power density in the absorption region. Only the fundamental mode exists in both the passive waveguide and the photodiode regions. Fig. 2 shows the optical field distribution of the VMDP in the photodiode region. Most of the optical energy is concentrated in the waveguide core. The optical absorption and the coupling loss per photodiode for the VMDP with 11μm long photodiodes and 89μm spacing between photodiodes are estimated to be 6.2% and 1.8%, respectively, by the BPM simulation. The coupling loss can be further improved by reducing the width of the active mesa.

Device characteristics: The finished devices are cleaved and mounted on copper heat sinks before testing. The VMDP exhibits a very low dark current: 190pA at 10V bias for individual photodiodes (11 × 48μm²), and 25nA for the 1.2mm long VMDP with 12 photodiodes. The excess dark current in the VMDP is attributed to the leakage current under the CPS electrodes, which has a much larger area than the active photodiodes. This can be eliminated by placing the electrodes on thin dielectric. The external quantum efficiency is measured to be 0.42A/W after anti-reflection (AR) coating. The dominant loss comes from the coupling from the optical fibre to the VMDP. All devices exhibit linear responsivity up to 12mA of photocurrent.

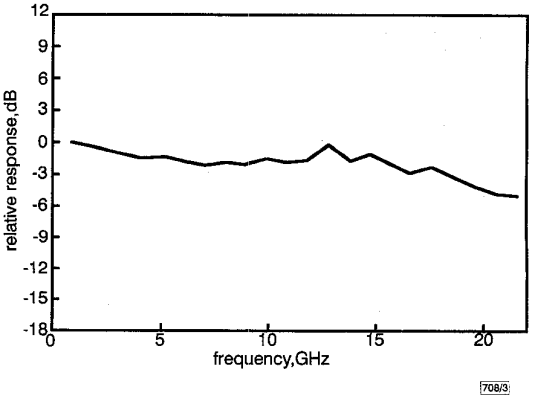

Fig. 3 *Measured frequency response of long wavelength VMDP*
12 photodiodes, total length = 1.2mm

The microwave performance of the VMDP is measured by an HP 8510C network analyser. The microwave return loss (S_{11}) is <−22dB from 0.1 to 40GHz. The characteristic impedance of the VMDP is matched very well to 50Ω (within 4%) for the entire frequency range. The frequency response of the VMDP is characterised by the optical heterodyne method [6, 7] using two external cavity tunable lasers at 1.55μm. The optical signals are combined by a 3dB coupler, and coupled to the VMDP through a fibre pickup head. The output microwave is collected by a 50GHz picoprobe (GGB Industries) and monitored by an RF power meter. The calibrated frequency response of the VMDP is shown in Fig. 3. A 3dB bandwidth of 18GHz is measured. The bandwidth is limited by the transit time of the MSM photodiodes. By scaling down the MSM to a 0.1μm scale, much higher bandwidth (> 100GHz) can be obtained.

The maximum photocurrent of 12mA is currently limited by thermal damage to the MSM photodiode. The device remains linear up to the maximum photocurrent. Inspection of the failed device by energy dispersive X-ray analysis (EDX) indicates that gold difflision into the semiconductor is the main failure mechanism. Improving the diffusion barrier of the Schottky contact should lead to even higher photocurrent.

Conclusion: We have experimentally demonstrated a long wavelength velocity-matched distributed photodetector with twelve metal-semiconductor-metal photodiodes. A 3dB bandwidth of 18GHz and an external quantum efficiency of 0.42A/W have been achieved.

Acknowledgments: This project is supported by TRW, ONR MURI on RF Photonics, NRAO, Tracor and HRL under UC MICRO and JSEP. The authors would like to thank Shi-Sheng Lee for help with figure editing.

27 May 1998
Electronics Letters Online No: 19980993

T. Chau, L. Fan, D.T.K. Tong, S. Mathai and M.C. Wu (*UCLA, Electrical Engineering Department, 66-147D Engineering IV, Box 951594, Los Angeles, CA 90095-1594, USA*)

E-mail: wu@ee.ucla.edu

D.L. Sivco and A.Y. Cho (*Lucent Technologies, Bell Laboratories, Murray Hill, NJ 07974, USA*)

References

1 LIN, L.Y., WU, M.C., ITOH, T., VANG, T.A., MULLER, R.E., SIVCO, D.L., and CHO, A.Y.: 'High-power high-speed photodetectors. Design, analysis, and experimental demonstration', *IEEE Trans. Microw. Theory Tech.*, 1997, **MTT-45**, pp. 1320–1331

2 JIANG, H., ZHU, J.T., KELLNER, A.L., YU, P.K.L., and LIU, Y.Z.: 'High-saturation-power waveguide photodetectors for analog fiber optic links'. Proc. SPIE, Photonics and Radio Frequency, Denver, Colorado, 7–8 August 1996, Vol. 2844, pp. 120–124

3 JASMIN, S., ENARD, A., RENAUD, J.-C., and VODJDANI, N.: 'High-speed high-power waveguide photodetector with distributed absorption'. Photonics and Radio Frequency, Denver, Colorado, 7–8 August 1996, Vol. 2844, pp. 125–132

4 COX, C.H., III: 'Gain and noise figure in analogue fiber-optic links', *IEE Proc. J, Optoelectron.*, 1992, **139**, pp. 238–242

5 CHAU, T., FAN, L., TONG, D.T.K., MATHAI, S., and WU, M.C.: 'Long wavelength velocity-matched distributed photodetectors'. IEEE Conf. on Lasers and Electro-Optics, San Francisco, CA, 3–8 May 1998

6 HAWKINS, T. II, JONES, M.D., PEPPER, S.H., and GOLL, J.H.: 'Comparison of fast photodetector response measurement by optical heterodyne and pulse response techniques', *J. Lightwave Technol.*, 1991, **9**, pp. 1289–1294

7 HALE, P.D., HUMPHREYS, D.A., and GIFFORD, A.D.: 'Photodetector frequency response measurements at NIST, US, and NPL, UK: preliminary results of a standards laboratory comparison'. SPIE, 1994, Vol. 2149, pp. 345–356

Optoelectronic clock recovery circuit using resonant tunnelling diode and uni-travelling-carrier photodiode

K. Murata, K. Sano, T. Akeyoshi, N. Shimizu, E. Sano, M. Yamamoto and T. Ishibashi

An optoelectronic clock recovery circuit is reported that monolithically integrates a resonant tunnelling diode and a uni-travelling-carrier photodiode. The integrated circuit extracts an electrical 11.55GHz clock signal from 11.55Gbit/s RZ optical data streams in a wide locking range with low power dissipation. Furthermore, the extraction of a subharmonic clock from 23.1 and 46.2Gbit/s input data streams is also confirmed.

Introduction: Because of the growth in multimedia services, ultra-high-speed optical receivers will be indispensable for future backbone networks. To realise a small high-speed receiver circuit with low power consumption, an optoelectronic circuit using resonant tunnelling diodes (RTDs), and a new type of wideband, high-saturation power photodetector called the uni-travelling-carrier photodiode (UTC-PD) [1] is a promising candidate because of its inherent high-speed operation. For example, an RTD/UTC-PD integrated circuit (IC) demultiplexing an 80Gbit/s optical signal into 40 Gbit/s electrical signals at an extremely low power of 7.75mW has been demonstrated [2]. A clock recovery circuit is another key component for realising the receiver circuit. Several kinds of optical injection-locked RTD oscillator [3 – 5] have been reported, and phase locking to optical input has been demonstrated. However, clock extraction from an optical data signal, such as a pseudo-random bit stream (PRBS), and subharmonic clock extraction have not been reported.

This Letter describes an optoelectronic clock recovery circuit that monolithically integrates an RTD and a UTC-PD on an InP substrate. The principle of synchronisation is optical injection-locking of a free-running oscillator. The fabricated circuit successfully extracted an electrical 11.55GHz clock signal from an 11.55Gbit/s RZ optical input data stream in a wide locking range with low power dissipation. Furthermore, the IC exhibited subharmonic clock extraction from 23.1Gbit/s and 46.2Gbit/s input data streams.

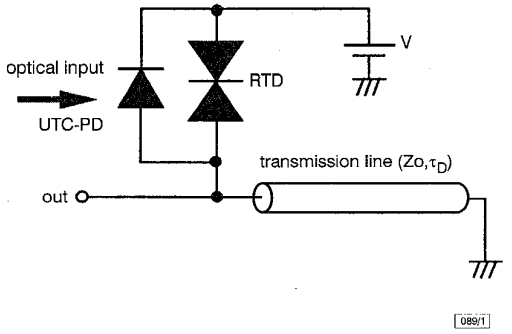

Fig. 1 *Circuit diagram of clock recovery circuit*

Circuit configuration: Fig. 1 shows a circuit diagram of the proposed clock recovery circuit. The circuit consists of an oscillator, which is constructed with an RTD and a transmission line, and a UTC-PD. In the RTD oscillator, the RTD is biased in the negative differential resistance (NDR) region, and the collector is connected to the transmission line whose other terminal is connected to the ground. The essential synchronisation principle is injection-locking of the RTD oscillator using the photocurrent generated by the UTC-PD. Here, the use of the UTC-PD is important to maintain fast photoresponse at low bias voltages [6] corresponding to the NDR region of the RTD. The self-oscillation of the RTD oscillator is theoretically analysed in [7], and the oscillating frequency is inversely proportional to the propagation delay time τ_D of the transmission line. In the present circuit, the transmission line is a coplanar wave guide monolithically fabricated on the InP substrate. The physical length and characteristic impedance Z_0 of the transmission line were 1150μm and 50Ω, respectively. The active areas of the RTD and UTC-PD were 6 and 20μm², respectively. The bias voltage V was +0.43V; the chip size was 1.9 × 0.5mm.

Experimental results: The IC was fabricated by monolithically integrating an InGaAs/AlAs/InAs RTD and an InP/InGaAs UTC-PD on an semi-insulating InP substrate [2, 8]. The peak and valley current of the RTD were 7.4mA at 0.35V and 0.6mA at 0.7V, respectively. The responsivity of the UTC-PD was 0.26A/W at a wavelength of 1.55μm, and the 3dB bandwidth around the bias voltage V was ~ 80GHz.

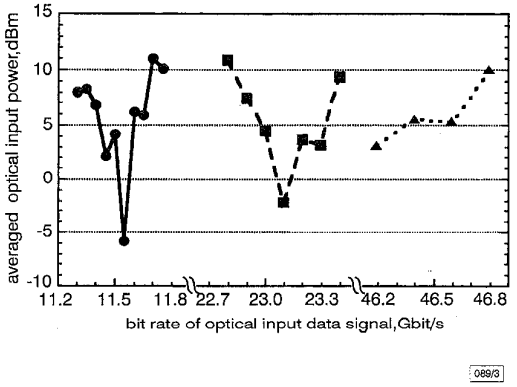

Fig. 3 *Locking range of clock recovery circuit*

● fundamental
■ first-order harmonic
▲ third-order harmonic

The IC was tested on a wafer. The input RZ optical data stream (λ = 1.55μm) was generated by an electro-optic pulse pattern generator that can output a 10–80Gbit/s optical data stream [9]. The pulsewidth of the RZ optical data input was < 10ps, and the data sequence was PN 2^{23}–1 PRBS. The input optical signal illuminated